Title

Tet3 regulates synaptic transmission and homeostatic plasticity via DNA oxidation and repair

Journal

Nature Neuroscience, 18(6)

ISSN

1097-6256

Authors

Yu, Huimei
Su, Yijing
Shin, Jaehoon
et al.

Publication Date

2015-06-01

DOI

10.1038/nn.4008

Peer reviewed

HHS Public Access

Author manuscript

Nat Neurosci. Author manuscript; available in PMC 2015 December 01.

Published in final edited form as:

Nat Neurosci. 2015 June ; 18(6): 836–843. doi:10.1038/nn.4008.

Tet3 regulates synaptic transmission and homeostatic plasticity via DNA oxidation and repair

Huimei Yu[1,2], **Yijing Su**[1,2], **Jaehoon Shin**[1,3], **Chun Zhong**[1,2], **Junjie U. Guo**[1,2,†], **Yi-Lan Weng**[1,2], **Fuying Gao**[6], **Daniel H. Geschwind**[6], **Giovanni Coppola**[6], **Guo-li Ming**[1,2,3,4,5], and **Hongjun Song**[1,2,3,4,*]

[1]Institute for Cell Engineering, Johns Hopkins University School of Medicine, 733 N. Broadway, Baltimore, MD 21205, USA.

[2]Department of Neurology, Johns Hopkins University School of Medicine, 733 N. Broadway, Baltimore, MD 21205, USA.

[3]Graduate Program in Cellular and Molecular Medicine, Johns Hopkins University School of Medicine, 733 N. Broadway, Baltimore, MD 21205, USA.

[4]The Solomon H. Snyder Department of Neuroscience, Johns Hopkins University School of Medicine, 733 N. Broadway, Baltimore, MD 21205, USA.

[5]Department of Psychiatry and Behavioral Sciences, Johns Hopkins University School of Medicine, 733 N. Broadway, Baltimore, MD 21205, USA.

[6]Semel Institute for Neuroscience and Human Genetics, and Program in Neurogenetics, Departments of Neurology and Psychiatry, David Geffen School of Medicine, University of California Los Angeles, Los Angeles, CA, USA.

Abstract

Contrary to the long-held belief that DNA methylation of terminally differentiated cells is permanent and essentially immutable, post-mitotic neurons exhibit extensive DNA demethylation. The cellular function of active DNA demethylation in neurons, however, remains largely unknown. Tet family proteins oxidize 5-methylcytosine to initiate active DNA demethylation through the base-excision repair pathway. Here, we show that synaptic activity bi-directionally regulates neuronal Tet3 expression. Functionally, knockdown of Tet or inhibition of base-excision

*Correspondence should be addressed to: Hongjun Song, Ph.D. Institute for Cell Engineering, Johns Hopkins University School of Medicine, 733 N. Broadway, MRB 759, Baltimore, MD 21205, USA shongju1@jhmi.edu.

†Present address: Whitehead Institute for Biomedical Research, Cambridge, MA 02142, USA.

AUTHOR CONTRIBUTIONS

H.Y. performed electrophysiological analyses. Y.S. performed biochemical and DNA methylation analyses. J.S. and J.U.G. performed bioinformatics analysis. C.Z. and Y.W. generated AAV. F.G., D.H.G., G.C. performed RNA-seq. G-l.M. and H.S. designed the project and wrote the manuscript.

GEO access number: GSE67245.

COMPETING FINANCIAL INTERESTS

The authors declare no competing financial interests.

Supplemental Information

Supplemental Information includes online methods, two tables and 11 figures.

repair in hippocampal neurons elevates excitatory glutamatergic synaptic transmission, whereas overexpressing Tet3 or Tet1 catalytic domain decreases it. Furthermore, dysregulation of Tet3 signalling prevents homeostatic synaptic plasticity. Mechanistically, Tet3 dictates neuronal surface GluR1 levels. RNA-seq analyses further revealed a pivotal role of Tet3 in regulating gene expression in response to global synaptic activity changes. Thus, Tet3 serves as a synaptic activity sensor to epigenetically regulate fundamental properties and meta-plasticity of neurons via active DNA demethylation.

INTRODUCTION

Emerging evidence supports critical roles of epigenetic modifications, including both histone and DNA modifications, in neuronal plasticity, learning and memory, and in neurological and psychiatric disorders[1-5]. Cytosine methylation is the predominant covalent modification of eukaryotic genomic DNA and regulates transcription in a highly cell type- and genomic context-dependent manner[6,7]. The notion that methylation of cytosine in the genomic DNA of terminally differentiated cells is largely irreversible has been overturned by demonstrations of the loss of cytosine methylation in non-proliferating cells, such as post-mitotic neurons[8-16]. In particular, genome-wide studies with the single-base resolution in neurons have revealed large-scale changes in DNA methylation status during development and in response to neuronal activity[14,15,17], suggesting that dynamic DNA methylation could make a functional contribution to these biological processes[2,4,5].

The functional role of neuronal DNA demethylation, however, is not well understood, because we had limited knowledge of its underlying molecular mechanisms. One breakthrough came from the identification of Ten-eleven translocation (Tet) family proteins (Tet1-3), which oxidize 5-methylcytosine (5mC) into 5-hydroxymethylcytosine (5hmC) to initiate the active DNA demethylation process[18,19]. Subsequent studies have shown that Tet-initiated active DNA demethylation is mediated through the base-excision DNA repair pathway in neurons[13] and in various other cell types[20,21]. The mammalian brain contains the highest 5hmC levels[22,23], which are dynamically regulated under physiological and pathological conditions[23,24]. Advances in our understanding of the molecular machinery mediating active DNA demethylation provide essential tools and an entry point to start to address the causal role of this pathway in neurons. Recent studies have revealed critical roles of Tet family members in activity-regulated neuronal gene expression[13] as well as memory formation and extinction[25-27]. Because Tet proteins are known to exhibit functions independent of DNA demethylation activity[28,29], it remains unclear whether DNA demethylation is directly required in these functions. In addition, cellular processes regulated by active DNA demethylation in neurons are completely unknown. Given that active DNA demethylation requires oxidation and subsequent excision repair of genomic DNA, a question remains as to whether and how a pathway that effectively culminates in an insult to the genome and potential disruption of genomic stability could be critical for recurrent cellular processes in post-mitotic neurons that exist for decades or a lifetime.

Here we investigated cellular functions of the Tet-mediated active DNA demethylation pathway in hippocampal neurons. We found that synaptic activity bi-directionally regulates

neuronal Tet3 expression, which in turn affects excitatory glutamatergic synaptic transmission via modulation of surface GluR1 levels. Furthermore, dysregulation of Tet3-mediated DNA demethylation signalling prevents homeostatic synaptic plasticity. RNA-seq analyses also showed a pivotal role of Tet3 in regulating gene expression in response to global synaptic activity changes. These results revealed a functional role of active DNA demethylation signalling as a synaptic activity sensor to regulate fundamental properties of neurons.

RESULTS

Activity-dependent expression of Tet3 regulates synaptic transmission

To identify the potential role of Tet proteins in neuronal function, we first characterized the expression of Tet family members in hippocampal neurons under basal conditions and upon changes of neuronal circuit activity. Quantitative PCR analysis showed that mRNA levels of Tet3, but not Tet1 and Tet2, were significantly increased upon elevating global synaptic activity in the presence of bicuculline (20 μM) and decreased upon reducing global synaptic activity in the presence of tetrodotoxin (TTX; 1 μM; Fig. 1a and Supplementary Table 1a). We confirmed Tet3 protein level changes at 4 hours after different treatments (Fig. 1b). These results established that neuronal Tet3 expression is bi-directionally regulated by changes in global synaptic activity.

Tet3 protein is localized in the nucleus of neurons (Supplementary Fig. 1a). To examine the impact of Tet3 expression in neurons, we used AAV to co-express EYFP and shRNAs against mouse Tet3 in cultured hippocampal neurons (Supplementary Fig. 1b and Supplementary Table 1b). shRNA-Tet3-1 and shRNA-Tet3-2[19], but not a control shRNA (sh-control), effectively reduced endogenous Tet3 expression in neurons at both mRNA and protein levels without any changes in Tet1 and Tet2 mRNA expression (Fig. 1b and Supplementary Fig. 1c). Dot-blot analyses showed no differences in global 5hmC levels in neurons with Tet3 knockdown (Tet3-KD; Supplementary Fig. 1d), likely due to the presence of Tet1 and Tet2 in these neurons. Whole-cell patch-clamp recording of $EYFP^+$ neurons also showed no significant differences in firing properties (Supplementary Fig. 1e). Immunocytochemistry analyses showed similar densities of synapsin I^+ synaptic boutons under different conditions (Supplementary Fig. 1f). Thus, Tet3 deficiency does not appear to generally affect global neuronal properties. Interestingly, electrophysiological recordings showed that Tet3-KD neurons, using two independent shRNAs, exhibited significantly larger amplitudes of miniature glutamatergic excitatory postsynaptic currents (mEPSCs), compared to those expressing sh-control (Fig. 1c). Conversely, neurons transfected with a construct co-expressing EYFP and Tet3 (Tet3 OE) exhibited significantly smaller mEPSC amplitudes compared to those expressing EYFP alone (Fig. 1d). Given that only less than 5% of neurons were transfected in these experiments, the effect of Tet3 overexpression is likely to be cell autonomous. Together, these results showed that neuronal Tet3 levels bi-directionally affect excitatory synaptic transmission.

Tet3 regulates synaptic transmission via DNA oxidation and repair

Given that these neurons express Tet1 and Tet2 at constant levels, we also examined the effect of Tet1 or Tet2 knockdown on synaptic transmission. We developed efficient shRNAs against Tet1 or Tet2 and AAV-mediated expression reduced Tet1 or Tet2 levels in these neurons, respectively (Supplementary Fig. 1c). Interestingly, neurons with decreased expression of either Tet1 or Tet2 also exhibited increased mEPSC amplitudes compared to those with sh-control, although the effect was modest in comparison to Tet3 KD (Fig. 2a). In addition, AAV-mediated overexpression of the catalytic domain of Tet1 (Tet1-CD), but not a dioxygenase-dead mutant[13] (Tet1-mCD), decreased mEPSC amplitudes (Fig. 2b), accompanied by increased total 5hmC levels (Supplementary Fig. 1d). Therefore, changes of DNA oxidation activity in neurons is sufficient to modulate basal levels of synaptic transmission.

Tet proteins are known to exhibit oxidation-independent functions in embryonic stem cells[28,29] and in neurons[25]. On the other hand, Tet-induced active, region-specific DNA demethylation is mediated by the base-excision repair (BER) pathway[13,30,31]. To further investigate the molecular mechanism by which Tet regulates synaptic transmission, we used two inhibitors of critical BER components, poly(ADP-ribose) polymerase inhibitor ABT-888 (ABT) and apurinic/apyrimidinic endonuclease inhibitor CRT0044876 (CRT), which have been shown to block DNA demethylation in mouse zygotes[32] and Tet1-CD-induced DNA demethylation in mammalian cells[13]. Treatment with ABT (50 μM) or CRT (50 μM) for 48 hours led to increased mEPSC amplitudes (Fig. 2c), resembling the Tet KD effect. Furthermore, the reduced mEPSC amplitude from Tet1-CD overexpression was normalized to the same level as those of control neurons upon CRT treatment, suggesting that BER functions downstream of DNA oxidation to regulate synaptic transmission (Fig. 2d). Together, these results suggest a model that Tet regulates basal levels of excitatory synaptic transmission in neurons through DNA oxidation and subsequent base-excision repair.

Tet3 is required for homeostatic synaptic plasticity

Given that Tet3 expression is bi-directionally regulated by TTX and bicuculline treatments (Fig. 1a), which are well-known to induce homeostatic synaptic scaling[33], we next focused on Tet3 to assess whether it also regulates synaptic plasticity. Notably, either Tet3 KD or BER inhibition elevated mEPSC amplitudes linearly across the spectrum under basal conditions (Supplementary Fig. 2a & 3a), which was comparable to the scaling-up effect induced by TTX treatment in normal neurons (Supplementary Fig. 2c). Therefore, downregulation of Tet3 signaling appeared to be sufficient to induce scaling-up. Importantly, Tet3 KD or BER inhibition showed no additional scaling-up upon TTX treatment (Fig. 3a-b and Supplementary Fig. 2b & 3b), indicating occlusion of these two manipulations. On the other hand, overexpression of Tet3 or Tet1-CD, but not Tet1-mCD, completely prevented TTX-induced scaling-up (Fig. 3c-d and Supplementary Fig. Fig. 4b-c & 5b-c), suggesting that downregulation of Tet signaling is required for scaling-up. Together, these results support a model that TTX treatment downregulates Tet3 signaling, which mediates homeostatic scaling-up of excitatory synaptic transmission.

Homeostatic synaptic scaling-up of excitatory synaptic transmission has also been shown to be induced by all-trans retinoic acid (RA)[34]. While acute RA treatment (1 μM) increased mEPSC amplitude of neurons expressing sh-control, there was no further increase in Tet3-KD neurons (Fig. 3e and Supplementary Fig. 2f-g), indicating that they also occlude each other. These results suggest that Tet3 signaling is required for different types of homeostatic synaptic plasticity.

Does bicuculline-induced Tet3 upregulation also regulate synaptic scaling-down? Indeed, neurons overexpressing Tet3 and Tet1-CD, but not Tet1-mCD, exhibited reduced mEPSC amplitudes linearly across the spectrum (Supplementary Fig. 4a & 5a), resembling bicuculline-induced scaling-down in normal neurons (Supplementary Fig. 4e). Up-regulating Tet3 signaling or oxidation activity via Tet1-CD also occluded bicuculline-induced scaling-down (Fig. 4a-b and Supplementary 4d-e & 5d-e). In addition, down-regulating Tet3 signaling via Tet3 KD or BER inhibition prevented bicuculline-induced scaling-down (Fig. 4c-d and Supplementary Figs. 2d-e & 3d-e). These results suggest that global synaptic activity modulates Tet3 expression and DNA demethylation activity, which in turn mediates homeostatic synaptic scaling-up or scaling-down.

Tet3 regulates synaptic transmission and plasticity via modulating surface GluR1 levels

A key cellular mechanism regulating both basal glutamatergic synaptic transmission and homeostatic scaling is the control of surface levels of glutamate receptors[35]. Quantitative immunocytochemistry analysis showed that Tet3-KD neurons exhibited elevated surface GluR1 levels; conversely, neurons overexpressing Tet1-CD, but not Tet1-mCD, displayed reduced surface GluR1 levels (Fig. 5a-b). Quantitative Western blot analyses also showed bi-directional changes of surface GluR1 levels (Fig. 5c), but not total GluR1 levels (Supplementary Fig. 6a). There was no significant change in either total or surface GluR2 levels upon Tet3 KD or Tet1-CD expression (Supplementary Fig. 7a). Consistent with a change of functional GluR1 levels at synapses, treatment of NASPM (1-Naphthyl acetyl spermine trihydrochloride), which blocks all GluR2-lacking AMPA receptors[36], led to a larger reduction of mEPSC amplitudes in Tet3-KD neurons than those neurons expressing sh-control (Supplementary Fig. 7b). Analysis of mESPC decay time under different conditions was also consistent with changes of GluR1 levels at synapses (Supplementary Fig. 7c). Together, these results support the model that Tet3 regulates basal excitatory synaptic transmission via regulating surface GluR1 levels.

This same cellular mechanism also explains the role of Tet3 in homeostatic synaptic scaling. Tet3 KD was sufficient to elevate surface GluR1 levels and prevent further changes upon TTX or bicuculline treatment (Fig. 5a, c). Conversely, overexpression of Tet1-CD was sufficient to reduce surface GluR1 levels and prevent further changes upon bicuculline or TTX treatment (Fig. 5b-c). Thus, changes in Tet3 signaling are both sufficient and necessary for the TTX-induced increase and bicuculline-induced decrease in surface GluR1 expression and resultant synaptic scaling. The immediate early gene, Arc, is known to regulate GluR insertion and synaptic scaling[37-39]. Interestingly, Tet3 KD led to decreased Arc protein levels, which mimics TTX–induced down regulation of Arc, and prevented bicuculline-induced Arc up-regulation (Supplementary Fig. 6b). Therefore, regulation of Arc levels

appears to explain changes in surface GluR1 levels upon Tet3 KD. Together, our results suggest a model that Tet3 and active DNA demethylation signalling respond to changes in global synaptic activity to re-establish a responsive cellular state.

Tet3 is essential for activity-induced gene expression changes and DNA demethylation

To further support this model and directly examine the role of Tet3 in synaptic activity-dependent gene expression, we performed RNA-seq analyses of sh-control and Tet3-KD neurons at 4 hours after saline, TTX, or bicuculline treatment (Supplementary Fig. 8 and Supplementary Table 2). RNA-seq confirmed 70% knockdown efficacy for Tet3 mRNA levels in neurons expressing sh-Tet3-2 (Supplementary Fig. 8a). At the basal level, Tet3-KD neurons exhibited differential expression of a large number of genes compared to those expressing sh-control, with more genes down-regulated than up-regulated (Fig. 6a and Supplementary Table 2b-g). Notably, many genes related to synapses and synaptic transmission were among differentially expressed genes (Supplementary Fig. 9). Multidimensional scaling, an unbiased method to quantify the degree of similarity between large data sets, showed clear segregation between sh-control and sh-Tet3-2 groups (Supplementary Fig. 8c). As expected, TTX or bicuculline treatments induced significant transcriptomic changes in neurons expressing sh-control, as shown by clear segregation among different groups (Supplementary Fig. 8c). In contrast, Tet3-KD neurons showed reduced segregation between saline and bicuculline treatment and no segregation between saline and TTX treatment (Supplementary Fig. 8c). Strikingly, among TTX-responsive genes in control neurons (FDR < 0.05), 99% of up-regulated and 85% of down-regulated genes lost responsiveness in Tet3-KD neurons (Fig. 6b). Among bicuculline-responsive genes in control neurons (FDR < 0.05), 77% of up-regulated and 94% of down-regulated genes lost responsiveness in Tet3-KD neurons, while very few genes were significantly up-regulated (8) or down-regulated (4) specifically in Tet3-KD neurons (Fig. 6b). Further analysis of up- and down-regulated genes in two separate populations showed that expression changes induced by TTX or bicuculline treatment were significantly attenuated in Tet3-KD neurons compared to those expressing sh-control (Fig. 6c). Notably, bicuculline-induced expression of immediate early genes, including *Arc*, *c-Fos*, *Npas4* and *Egr4*, was largely unaffected in Tet3-KD neurons when examined at 4 hours after treatment (Supplementary Fig. 10a), suggesting no general impairment of Tet3-KD neurons in response to neuronal activation. Taken together, these results identified an essential role of Tet3 in regulating gene expression in response to changes of global synaptic activity.

To ascertain that Tet3 can directly regulate gene expression via active DNA demethylation, we focused on brain-derived neurotrophic factor (*Bdnf*), a gene that has been shown to exhibit active DNA demethylation in these neurons[8] and has been implicated in regulating both excitatory synaptic transmission[40] and synaptic scaling[41]. Bisulfite sequencing analysis showed that Tet3-KD neurons exhibited increased CpG methylation at the *Bdnf* promoter IV region, whereas overexpressing Tet1-CD had the opposite effect (Fig. 7a-b and Supplementary Table 1c). Consistent with a lack of global changes in DNA methylation levels (Supplementary 1d), Tet3 KD did not affect CpG methylation at the *Fgf1G* promoter region (Fig. 7a-b), or promoters of *Arc* and *Npas4* (Supplementary Fig. 10b). ChIP-PCR analysis further showed an association of Tet3 with the *Bdnf IV* region, but not the *Fgf1G*

region, in neurons (Fig. 7c and Supplementary Table 1d). Upon TTX-induced decreases in global synaptic activity and Tet3 expression, CpG methylation at the *Bdnf IV* region was significantly increased (Fig. 7a-b). Conversely, bicuculline treatment increased Tet3 expression and decreased methylation at the same region (Fig. 7a-b). Accompanying methylation changes, neurons exhibited changes in *Bdnf IV* expression of the opposite direction (Fig. 7d). No changes in *Fgf1G* expression were detected under any conditions (Fig. 7d). Importantly, neurons with Tet3 KD or Tet1-CD overexpression exhibited no further changes in either methylation levels or mRNA expression of *Bdnf IV* upon TTX or bicuculline treatment (Fig. 7a-b & d). Taken together, these results support a critical role of Tet3 in regulating region-specific DNA demethylation and gene expression in response to global synaptic activity changes.

DISCUSSION

Our study identified Tet3 as a novel global synaptic activity sensor and demonstrated that, surprisingly, even the most fundamental properties of neurons, such as synaptic transmission and surface GluR1 levels, are dynamically regulated via DNA oxidation and subsequent base-excision repair. Active DNA demethylation thus plays a much broader and fundamental role in neurons than previously recognized. While studies of neuronal DNA damage and repair have traditionally focused on their roles in stress, aging, degenerative neurological disorders, and other pathophysiological conditions[42], our results suggest a previously underappreciated role for DNA repair in normal neuronal physiology and plasticity.

Tet3 has been shown to regulate zygotic paternal DNA reprogramming[43-45] and embryonic neural development[46,47]. Recent studies have also shown that Tet1 regulates expression of some neuronal genes and mouse behavior related to learning and memory[25,26,48]. Using genetic and pharmacological approaches, we not only identified physiological functions of Tet3 in neurons, but also pinpointed the underlying mechanism involving DNA oxidation and active DNA demethylation signaling. Our results suggest a pivotal role of Tet3 in regulating gene expression in response to global synaptic activity changes. Although it is unlikely that all these genes are directly regulated by Tet3, we identified one *bona fide* target *Bdnf*, which is known to regulate synaptic transmission and scaling[41]. Interestingly, activity-induced expression of immediate early genes *Arc*, *c-Fos*, *Npas4* and *Egr4* requires the function of Tet1[25,26], but not Tet3 (Supplementary Fig. 10a). In addition, Tet1-deficient neurons exhibit hypermethylation at *Arc* and *Npas4* promoters[26], which was not the case for Tet3-KD neurons (Supplementary Fig. 10b). On the other hand, all Tets regulate basal levels of synaptic transmission. Together, these results suggest that Tet family members could have shared, but also distinct roles in neurons.

Homeostatic plasticity allows neurons to sense how active they are and to adjust their properties to maintain stable firing[33]. We showed that changes in Tet3 expression and DNA demethylation activity mediate both synaptic scaling-up and scaling-down via a classic pathway through Arc and GluR1 surface level regulation. Our results are consistent with previous findings of the requirement for gene transcription in TTX-induced synaptic scaling-up[49] and further describe an unexpected underlying mechanism via DNA oxidation and

repair. In a classic view, the major role of epigenetic DNA methylation is to maintain cell identity. Our results significantly extend this view and suggest that, in non-dividing cells, the active DNA demethylation pathway dynamically responds to and processes external stimuli to establish a new cellular state. We provide one example in the nervous system for a critical role of active DNA demethylation in meta-plasticity, a phenomenon in which the history of a neuron's activity determines its current state and its ability to undergo synaptic plasticity[50].

Beyond advancing our understanding of the functions of Tet3 in regulating neuronal properties and gene expression, our study provides the first genetic evidence for a causal role of DNA oxidation and active demethylation in regulating synaptic transmission, which is fundamental to all basic and higher-order information processing essential for brain functions. Therefore, our findings have broad implications for understanding epigenetic regulation of the nervous system under physiological and pathological conditions.

ONLINE METHODS

Hippocampal neuronal culture, expression constructions, and genetic and pharmacological manipulations

Primary hippocampal neurons were prepared as previously described[11,51]. Briefly, hippocampi were dissected from E16.5-17.5 mouse embryos (C57BL/6) and dissociated neurons were plated on poly-lysine coated coverslips in Neurobasal-A medium supplemented with B27 (Invitrogen). AAV gene delivery vectors were constructed by cloning the EF1a-Gene-WPRE cassette[52] into an AAV backbone by SalI and ECoRV. The shRNA sequences used were listed in Supplementary Table 1b. The shRNAs against mouse Tet1, 2, 3 have been previously characterized[13,19] and we further confirmed their efficacy in primary hippocampal neurons by QPCR (Supplementary Fig. 1c) and Western blot analyses (Fig. 1b). Mouse Tet3 cDNA was used for overexpression analysis. AAV-Tet1-CD and AAV-Tet1-mCD has been previously characterized[13]. For AAV-mediated genetic manipulations, engineered AAV co-expressing EYFP or transgenes and shRNA were added into the culture medium at DIV 1 (day *in vitro*). Over 99% cells were infected based on EYFP or transgene expression. Tet3 cDNA was too large for AAV packaging and was directly co-transfected with EYFP cDNA into neurons with Lipofectamine 2000 (Invitrogen) at DIV 4-5. Less than 5% of neurons were transfected based on EYFP expression. For pharmacological treatments, vehicle, ABT (50 μM) or CRT (50 μM) was applied for 48 hours and RA (1 μM) was applied for 2 hours before analyses. All analyses were performed at DIV 8-9. Synaptic scaling experiments were performed as previously described[53]. Cultures were treated with 1 μM TTX or 20 μM bicuculline for 48 hours and then subjected to electrophysiological analyses of mEPSCs, immunocytochemistry or Western blot analysis of surface and total GluR1 or GluR2 levels, or dot blot analysis of total 5hmC levels.

Quantitative real-time reverse transcription PCR, and mRNA-sequencing and analyses

For gene expression analysis, cultured hippocampal neurons were treated with saline, 1 μM TTX or 20 μM bicuculline for 4 hours in parallel cultures and total RNA was purified using

RNeasy Mini Kit (Qiagen Inc). Quantitative real-time PCR was performed with two steps SYBR Green Supermix (ABI). Specific primers (Supplementary Table 1a) were used to measure the expression level of target genes with the ΔΔCt method as previously described[13].

RNA-seq analysis was performed as previously described[54]. A total of 17 samples from parallel cultures 4 hours after different treatment were used. Sequencing libraries were prepared using Illumina Truseq RNA sample prep kit following manufacturer's protocol. Briefly, total RNA was poly-A tail selected and then heat fragmented. The fragmented RNA was reverse transcribed and the second strand was synthesized to make double stranded DNA. After end repair and 3' adenylation, adapters for multiplexing were ligated to the end of double stranded DNA fragments. The ligation products were amplified and purified to generate Illumina compatible libraries. Sequencing was performed with 50bp-paired end multiplexed sequencing by Illumina Hiseq2500. The raw reads were mapped to the mouse genome build mm9 using tophat[55]. The differential expression was called by cuffdiff[56] with a default FDR of 0.05. Downstream analyses were performed using the Bioconductor EdgeR package[57] and custom R scripts.

Electrophysiological analysis

Whole-cell patch-clamp recordings (V_m = -70 mV) were performed from hippocampal cultures at the DIV 8-9 as previously described[58]. Briefly, micro-pipettes (World Instruments, Inc.) with 3-7 MΩ resistance were filled with the following internal solution (in mM): K-gluconate 130, KCl 4, HEPES 10, EGTA 2, ATP 4, GTP 0.3, and phosphocreatine 7 (pH 7.3). The following external solution (in mM) was used: NaCl 140, KCl 3, $CaCl_2$ 2, $MgCl_2$ 1.3, HEPES 10, and glucose 10 (pH 7.4). For voltage-clamp recordings of mEPSC, 1 μM TTX and 20 μM bicuculline were added to the external solution. Axopatch 200B amplifier (Axon Instruments), Digidata 1322A analog-to-digital converted (Axon Instruments) and pCLAMP 9 software (Axon Instruments) were used for data acquisition. All data was filtered with a lowpass Bessel filter at a frequency of 2 kHz and stored at 5 kHz. pCLAMP 9 and Minianalysis software (Synaptosoft Inc.) was used for analysis. All experiments were performed in parallel from the same preparation.

Bisulfite sequencing analysis, 5hmC dot blot and ChIP-PCR analyses

Bisulfite sequencing analysis was performed as previously described[11]. Briefly, bisulfite (Zymo Research)-treated DNA was used as a template for PCR amplification of region of interest with specific primers (Supplementary Table 1c). PCR products were gel-purified and cloned into pCR 2.1 TA (Invitrogen) vector. Individual clones were sequenced and aligned with the reference sequence. A minimal of 15 alleles were examined for each sample and three independent experiments were performed for each condition to obtain mean ± s.e.m.

Dot blot analysis of 5hmC was performed as previously described[13]. Briefly, genomic DNA samples from different treated groups were adjusted to a concentration of 100 ng/μl, heat-denatured at 95°C for 5 minutes, and chilled on ice for 1 minute. Each sample of 0.1 μg DNA was applied onto a piece of Hybond-N+ membrane (Amersham), then cross-linked by

a UV stratalinker 1800 (Stratagene). Membranes were blocked by 5% dry milk, and then incubated with antibodies (1:10000 for anti-5hmC; Active motif). Signal was visualized by a HRP-conjugated donkey anti-rabbit IgG antibodies (Santa Cruz) and SuperSignal West Pico Chemiluminescent Substrate (Thermoscientific).

Chromatin immunoprecipitation analysis was performed as previously described[11]. Briefly, FLAG-Ctrl or FLAG-Tet3 overexpression constructs were electroporated into hippocampal neurons before plating (Amaxa) and cultures were subjected to ChIP at DIV 8 using anti-FLAG antibody (Sigma) following manufacture's instruction. Specific primers (Supplementary Table 1d) were used in PCR to detect the presence of specific DNA binding to Tet3.

Immunocytochemistry, surface biotinylation and Western blot analysis

Immunocytochemistry of cultured hippocampal neurons was performed as previously described[58]. Briefly, cells were fixed in 4% paraformaldehyde, subsequently permeabilized with 0.2% Triton X-100 in PBS for 10 minutes, then blocked for 1 hour in 10% normal donkey serum. Primary antibodies were incubated with neurons overnight at 4°C, including GFP (Millipore, MAB1083; 1:1000), Tuj1 (Millipore, MAB5564; 1:2000), and synapsin I (Millipore, 574777; 1:2000). Alexa 488, Alexa 555, or Alexa 647-conjugated secondary antibodies (Molecular Probes; 1:500) to appropriate species were incubated at room temperature for 2 hours. To label surface GluR1, 2.5 μg of N-terminal GluR1 antibody (Millipore, 07-660; 1:1000) was added to media and incubated at 10°C for 30 minutes. The unbound excess antibody was quickly washed with fresh medium and then fixed and mounted according to the methods described above. All immunocytochemistry experiments were performed from at least three individual batches of cultures for different conditions in parallel. Images were acquired by confocal microscopy (Zeiss 710) using identical settings for parallel cultured and quantified using ImageJ as previously described[59].

Surface biotinylation was performed as described previously[37]. Briefly, high density primary cultured cortical neurons were cooled on ice, washed twice with ice-cold PBS containing 1 mM $CaCl_2$ and 0.5 mM $MgCl_2$, and then incubated with 1 mg/ml Sulfo-NHS-SS-Biotin (Pierce) for 30 minutes at 4°C on a shaker with a gentle speed. The cells were washed three times with ice-cold Quenching solution (100 mM Glycine, pH 7.4) to quench the excess biotin before harvesting the proteins in RIPA buffer. Homogenates were centrifuged at 16,000 g for 20 minutes at 4°C. The supernatants were collected, 10% of total volume was saved for total protein analysis. The remaining 90% of the supernatants was incubated with Streptavidin beads (Pierce), and rotated at 4°C overnight. Precipitates were washed with RIPA buffer three times before heating at 98°C in SDS-PAGE loading buffer. Surface and total levels of GluRs were analyzed by immunoblotting with N-terminal GluR1 antibody (Millipore, 07-660; 1:1000) or GluR2 antibodies (Millipore, MAB397; 1:1000).

Westernblot analysis was performed as previously described[59]. Briefly, protein samples were separated by SDS-PAGE and gels were transferred to polyvinyl difluoride membranes (Millipore Corporation) for immunoblot analysis. Blots were incubated in blocking buffer (5% bovine Milk and 0.1% Tween 20 in PBS, pH 7.4) for 1 hour and then in specific primary antibodies overnight at 4°C, washed in blocking buffer three times for 10 minutes

each, and incubated in corresponding secondary antibodies at room temperature for 2 hours. The following antibodies were used: GluR1-N (Millipore, 07-660; 1:1000), Tet3 (gift of Dr. Guoliang Xu[43] and Abiocode, M1092-3; 1:3000) Membranes were stripped and re-blotted with mouse anti-Actin antibodies (Millipore, MAB1501; 1:3000) as loading control. Western blot images were analyzed by ImageJ. Statistical significance was determined by ANOVA.

Statistics

No statistical methods were used to pre-determine sample sizes but our sample sizes are similar to those generally employed in the field. No randomization and blinding were employed. A supplementary methods checklist is available.

Supplementary Material

Refer to Web version on PubMed Central for supplementary material.

ACKNOWLEDGEMENTS

We thank R. Huganir, P. Worley, G.C. Turrigiano, L. Chen for suggestions, members of Ming and Song laboratories for help and critical comments, G.L. Xu for Tet3 antibodies, L. Liu, Q. Hussaini, and Y. Cai for technical support. This work was supported by NIH (NS047344 to H.S; NS048271 and MH105128 to G.L.M.; NS062691 to D.G.), a grant from the Simons Foundation (SFARI240011 to H.S.), Brain & Behavior Research Foundation (BBRF; to H.S., G.L.M., and Y.S.), Maryland Stem Cell Research Foundation (to G.L.M. and H.S.), and by the Dr. Miriam and Sheldon G. Adelson Medical Research Foundation (to G.L.M., D.G., and G.C.). J.S. was supported by a Samsung fellowship.

REFERENCES

1. Tsankova N, Renthal W, Kumar A, Nestler EJ. Epigenetic regulation in psychiatric disorders. Nature reviews. Neuroscience. 2007; 8:355–367. [PubMed: 17453016]
2. Graff J, Kim D, Dobbin MM, Tsai LH. Epigenetic regulation of gene expression in physiological and pathological brain processes. Physiol Rev. 2011; 91:603–649. [PubMed: 21527733]
3. Telese F, Gamliel A, Skowronska-Krawczyk D, Garcia-Bassets I, Rosenfeld MG. “Seq-ing” insights into the epigenetics of neuronal gene regulation. Neuron. 2013; 77:606–623. [PubMed: 23439116]
4. Shin J, Ming GL, Song H. DNA modifications in the mammalian brain. Philosophical transactions of the Royal Society of London. Series B, Biological sciences. 2014; 369 doi:10.1098/rstb.2013.0512.
5. Day JJ, Kennedy AJ, Sweatt JD. DNA methylation and its implications and accessibility for neuropsychiatric therapeutics. Annual review of pharmacology and toxicology. 2015; 55:591–611. doi:10.1146/annurev-pharmtox-010814-124527.
6. Bird A. DNA methylation patterns and epigenetic memory. Genes Dev. 2002; 16:6–21. [PubMed: 11782440]
7. Law JA, Jacobsen SE. Establishing, maintaining and modifying DNA methylation patterns in plants and animals. Nat Rev Genet. 2010; 11:204–220. [PubMed: 20142834]
8. Martinowich K, et al. DNA methylation-related chromatin remodeling in activity-dependent BDNF gene regulation. Science. 2003; 302:890–893. [PubMed: 14593184]
9. Miller CA, Sweatt JD. Covalent modification of DNA regulates memory formation. Neuron. 2007; 53:857–869. [PubMed: 17359920]
10. Nelson ED, Kavalali ET, Monteggia LM. Activity-dependent suppression of miniature neurotransmission through the regulation of DNA methylation. The Journal of neuroscience : the official journal of the Society for Neuroscience. 2008; 28:395–406. [PubMed: 18184782]

11. Ma DK, et al. Neuronal activity-induced Gadd45b promotes epigenetic DNA demethylation and adult neurogenesis. Science. 2009; 323:1074–1077. [PubMed: 19119186]
12. Feng J, et al. Dnmt1 and Dnmt3a maintain DNA methylation and regulate synaptic function in adult forebrain neurons. Nat Neurosci. 2010; 13:423–430. [PubMed: 20228804]
13. Guo JU, Su Y, Zhong C, Ming GL, Song H. Hydroxylation of 5-methylcytosine by TET1 promotes active DNA demethylation in the adult brain. Cell. 2011; 145:423–434. [PubMed: 21496894]
14. Guo JU, et al. Neuronal activity modifies the DNA methylation landscape in the adult brain. Nature neuroscience. 2011; 14:1345–1351. [PubMed: 21874013]
15. Lister R, et al. Global epigenomic reconfiguration during mammalian brain development. Science. 2013; 341:1237905. doi:10.1126/science.1237905. [PubMed: 23828890]
16. Guo JU, Su Y, Zhong C, Ming GL, Song H. Emerging roles of TET proteins and 5-hydroxymethylcytosines in active DNA demethylation and beyond. Cell Cycle. 2011; 10:2662–2668. [PubMed: 21811096]
17. Guo JU, et al. Genome-wide antagonism between 5-hydroxymethylcytosine and DNA methylation in the adult mouse brain. Front Biol (Beijing). 2014; 9:66–74. doi:10.1007/s11515-014-1295-1. [PubMed: 25568643]
18. Tahiliani M, et al. Conversion of 5-methylcytosine to 5-hydroxymethylcytosine in mammalian DNA by MLL partner TET1. Science. 2009; 324:930–935. [PubMed: 19372391]
19. Ito S, et al. Role of Tet proteins in 5mC to 5hmC conversion, ES-cell self-renewal and inner cell mass specification. Nature. 2010; 466:1129–1133. [PubMed: 20639862]
20. Pollen AA, et al. Low-coverage single-cell mRNA sequencing reveals cellular heterogeneity and activated signaling pathways in developing cerebral cortex. Nat Biotechnol. 2014; 32:1053–1058. doi:10.1038/nbt.2967. [PubMed: 25086649]
21. Pastor WA, Aravind L, Rao A. TETonic shift: biological roles of TET proteins in DNA demethylation and transcription. Nature reviews. Molecular cell biology. 2013; 14:341–356. doi: 10.1038/nrm3589. [PubMed: 23698584]
22. Kriaucionis S, Heintz N. The nuclear DNA base 5-hydroxymethylcytosine is present in Purkinje neurons and the brain. Science. 2009; 324:929–930. [PubMed: 19372393]
23. Szulwach KE, et al. 5-hmC-mediated epigenetic dynamics during postnatal neurodevelopment and aging. Nature neuroscience. 2011; 14:1607–1616. [PubMed: 22037496]
24. Yao B, et al. Genome-wide alteration of 5-hydroxymethylcytosine in a mouse model of fragile X-associated tremor/ataxia syndrome. Human molecular genetics. 2014; 23:1095–1107. doi: 10.1093/hmg/ddt504. [PubMed: 24108107]
25. Kaas GA, et al. TET1 controls CNS 5-methylcytosine hydroxylation, active DNA demethylation, gene transcription, and memory formation. Neuron. 2013; 79:1086–1093. doi:10.1016/j.neuron.2013.08.032. [PubMed: 24050399]
26. Rudenko A, et al. Tet1 is critical for neuronal activity-regulated gene expression and memory extinction. Neuron. 2013; 79:1109–1122. doi:10.1016/j.neuron.2013.08.003. [PubMed: 24050401]
27. Todarello G, et al. Incomplete penetrance of NRXN1 deletions in families with schizophrenia. Schizophrenia research. 2014; 155:1–7. doi:10.1016/j.schres.2014.02.023. [PubMed: 24680031]
28. Williams K, et al. TET1 and hydroxymethylcytosine in transcription and DNA methylation fidelity. Nature. 2011; 473:343–348. [PubMed: 21490601]
29. Chen Q, Chen Y, Bian C, Fujiki R, Yu X. TET2 promotes histone O-GlcNAcylation during gene transcription. Nature. 2013; 493:561–564. [PubMed: 23222540]
30. Ito S, et al. Tet proteins can convert 5-methylcytosine to 5-formylcytosine and 5-carboxylcytosine. Science. 2011; 333:1300–1303. [PubMed: 21778364]
31. He YF, et al. Tet-mediated formation of 5-carboxylcytosine and its excision by TDG in mammalian DNA. Science. 2011; 333:1303–1307. [PubMed: 21817016]
32. Hajkova P, et al. Genome-wide reprogramming in the mouse germ line entails the base excision repair pathway. Science. 2010; 329:78–82. [PubMed: 20595612]
33. Turrigiano GG. The self-tuning neuron: synaptic scaling of excitatory synapses. Cell. 2008; 135:422–435. [PubMed: 18984155]

34. Aoto J, Nam CI, Poon MM, Ting P, Chen L. Synaptic signaling by all-trans retinoic acid in homeostatic synaptic plasticity. Neuron. 2008; 60:308–320. doi:10.1016/j.neuron.2008.08.012. [PubMed: 18957222]
35. Lee HK. Ca-permeable AMPA receptors in homeostatic synaptic plasticity. Frontiers in molecular neuroscience. 2012; 5:17. doi:10.3389/fnmol.2012.00017. [PubMed: 22347846]
36. Koike M, Iino M, Ozawa S. Blocking effect of 1-naphthyl acetyl spermine on Ca(2+)-permeable AMPA receptors in cultured rat hippocampal neurons. Neuroscience research. 1997; 29:27–36. [PubMed: 9293490]
37. Shepherd JD, et al. Arc/Arg3.1 mediates homeostatic synaptic scaling of AMPA receptors. Neuron. 2006; 52:475–484. doi:10.1016/j.neuron.2006.08.034. [PubMed: 17088213]
38. Gao M, et al. A specific requirement of Arc/Arg3.1 for visual experience-induced homeostatic synaptic plasticity in mouse primary visual cortex. The Journal of neuroscience : the official journal of the Society for Neuroscience. 2010; 30:7168–7178. [PubMed: 20505084]
39. Rial Verde EM, Lee-Osbourne J, Worley PF, Malinow R, Cline HT. Increased expression of the immediate-early gene arc/arg3.1 reduces AMPA receptor-mediated synaptic transmission. Neuron. 2006; 52:461–474. doi:10.1016/j.neuron.2006.09.031. [PubMed: 17088212]
40. Poo MM. Neurotrophins as synaptic modulators. Nature reviews. Neuroscience. 2001; 2:24–32. [PubMed: 11253356]
41. Rutherford LC, Nelson SB, Turrigiano GG. BDNF has opposite effects on the quantal amplitude of pyramidal neuron and interneuron excitatory synapses. Neuron. 1998; 21:521–530. [PubMed: 9768839]
42. Madabhushi R, Pan L, Tsai LH. DNA damage and its links to neurodegeneration. Neuron. 2014; 83:266–282. doi:10.1016/j.neuron.2014.06.034. [PubMed: 25033177]
43. Gu TP, et al. The role of Tet3 DNA dioxygenase in epigenetic reprogramming by oocytes. Nature. 2011; 477:606–610. [PubMed: 21892189]
44. Shen L, et al. Tet3 and DNA replication mediate demethylation of both the maternal and paternal genomes in mouse zygotes. Cell stem cell. 2014; 15:459–470. doi:10.1016/j.stem.2014.09.002. [PubMed: 25280220]
45. Guo F, et al. Active and passive demethylation of male and female pronuclear DNA in the Mammalian zygote. Cell stem cell. 2014; 15:447–458. doi:10.1016/j.stem.2014.08.003. [PubMed: 25220291]
46. Xu Y, et al. Tet3 CXXC domain and dioxygenase activity cooperatively regulate key genes for Xenopus eye and neural development. Cell. 2012; 151:1200–1213. [PubMed: 23217707]
47. Hahn MA, et al. Dynamics of 5-hydroxymethylcytosine and chromatin marks in Mammalian neurogenesis. Cell Rep. 2013; 3:291–300. [PubMed: 23403289]
48. Zhang RR, et al. Tet1 regulates adult hippocampal neurogenesis and cognition. Cell Stem Cell. 2013; 13:237–245. [PubMed: 23770080]
49. Ibata K, Sun Q, Turrigiano GG. Rapid synaptic scaling induced by changes in postsynaptic firing. Neuron. 2008; 57:819–826. [PubMed: 18367083]
50. Abraham WC, Bear MF. Metaplasticity: the plasticity of synaptic plasticity. Trends in neurosciences. 1996; 19:126–130. [PubMed: 8658594]
51. Song H, Stevens CF, Gage FH. Astroglia induce neurogenesis from adult neural stem cells. Nature. 2002; 417:39–44. [PubMed: 11986659]
52. Ge S, et al. GABA regulates synaptic integration of newly generated neurons in the adult brain. Nature. 2006; 439:589–593. [PubMed: 16341203]
53. Turrigiano GG, Leslie KR, Desai NS, Rutherford LC, Nelson SB. Activity-dependent scaling of quantal amplitude in neocortical neurons. Nature. 1998; 391:892–896. [PubMed: 9495341]
54. Jang MH, et al. Secreted frizzled-related protein 3 regulates activity-dependent adult hippocampal neurogenesis. Cell stem cell. 2013; 12:215–223. [PubMed: 23395446]
55. Trapnell C, Pachter L, Salzberg SL. TopHat: discovering splice junctions with RNA-Seq. Bioinformatics. 2009; 25:1105–1111. doi:10.1093/bioinformatics/btp120. [PubMed: 19289445]

56. Trapnell C, et al. Transcript assembly and quantification by RNA-Seq reveals unannotated transcripts and isoform switching during cell differentiation. Nat Biotechnol. 2010; 28:511–515. [PubMed: 20436464]

57. Robinson MD, McCarthy DJ, Smyth GK. edgeR: a Bioconductor package for differential expression analysis of digital gene expression data. Bioinformatics. 2010; 26:139–140. doi: 10.1093/bioinformatics/btp616. [PubMed: 19910308]

58. Song HJ, Stevens CF, Gage FH. Neural stem cells from adult hippocampus develop essential properties of functional CNS neurons. Nature neuroscience. 2002; 5:438–445. [PubMed: 11953752]

59. Kim JY, et al. DISC1 regulates new neuron development in the adult brain via modulation of AKT-mTOR signaling through KIAA1212. Neuron. 2009; 63:761–773. [PubMed: 19778506]

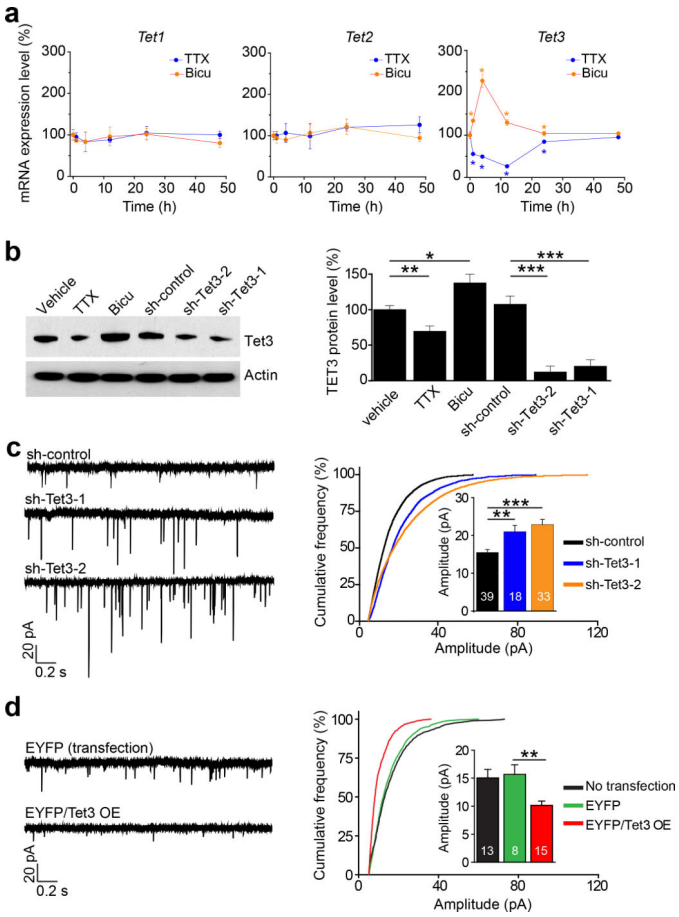

Figure 1.

Synaptic activity-dependent expression of Tet3 regulates glutamatergic synaptic transmission. (**a**) Expression of Tet family members in response to changes of global synaptic activity. Shown are summaries of time-course analysis of mRNA expression of Tet1, 2, 3 in cultured mouse hippocampal neurons after continuous presence of TTX (1 μM) or bicuculline (20 μM). The same cultures were used for analysis of expression of three Tet genes and data was normalized to time zero for parallel cultures. Values represent mean ± s.e.m. (n = 3; *P < 0.05, ANOVA; For Tet3 plot of TTX treatment, P = 0.5 at 0 h; P = 0.00007 at 1 h; P = 0.003 at 4 h; P = 0.002 at 12 h; P = 0.03 at 24 h and P = 0.07 at 48 h; For Tet2 bucuculline treatment: P = 0.5 at 0 h; P = 0.02 at 1 h; P = 0.01 at 4 h; P = 0.006 at 12 h; P = 0.02 at 24 h and P = 0.50 at 48 h,). (**b**) Western blot analysis of neuronal Tet3 protein levels upon different treatments. Hippocampal neurons in culture were treated with saline, TTX (1 μM) or bicuculline (20 μM) for 4 hours, or infected with AAV to express control shRNA (sh-control), or two different shRNAs against mouse Tet3 (sh-Tet3-1, -2). Shown are cropped sample Western blot images (left; full-length blots are presented in Supplementary Figure 11) and quantification of Tet3 protein levels (right). Values represent mean ± s.e.m. (n = 3; ***P < 0.001; **P < 0.01; *P < 0.05; ANOVA; P = 0.006, vehicle vs TTX; P = 0.02, vehicle vs Bicuculline; P = 0.0002, sh-control vs sh-Tet3-2; P = 0.0003, sh-control vs sh-Tet3-1). (**c**) Tet3-KD neurons exhibit elevated glutamatergic synaptic transmission. Shown are sample whole-cell voltage-clamp recording traces of hippocampal

neurons co-expressing EYFP and different shRNAs (left) and cumulative distribution plot of mESPC amplitudes (right). Shown in the inset is a summary of mean mESPC amplitudes. Numbers in bar graphs indicate numbers of neurons examined. Values represent mean ± s.e.m. (***$P < 0.001$; **$P < 0.01$; Kolmogorov-Smirnov test; $P = 0.003$, sh-control vs sh-Tet3-1; $P = 0.000009$, sh-control vs sh-Tet3-2). (**d**) Neurons overexpressing Tet3 exhibit decreased glutamatergic synaptic transmission. Same as in (**c**), except that neurons were transfected with vectors to express EYFP or co-express EYFP and Tet3 (Tet3 OE). Values represent mean ± s.e.m. (**$P < 0.01$; Kolmogorov-Smirnov test; $P = 0.002$, EYFP vs Tet3 OE).

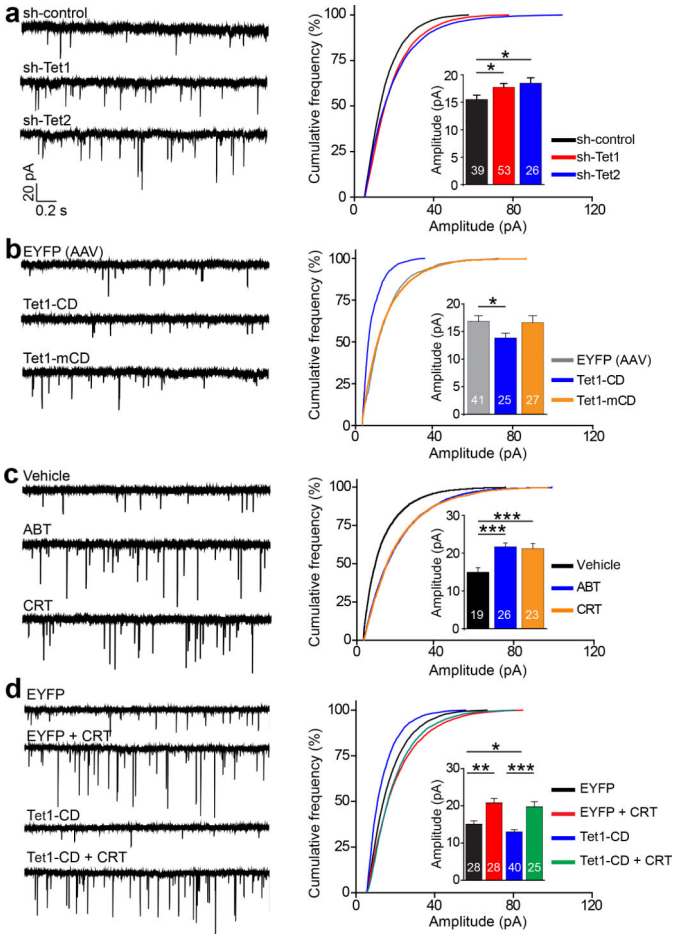

Figure 2.

DNA oxidation and base-excision repair regulates glutamatergic synaptic transmission. Same as in **Fig. 1c-d**, except that neurons were infected with AAV to co-express EYFP and shRNA against Tet1 or Tet2 (**a**), Tet1-CD or its enzymatic dead mutant (Tet1-mCD) (**b**), or treated with vehicle, ABT (50 μM), or CRT (50 μM), for 48 hours before analysis (**c-d**). Values represent mean ± s.e.m. (***$P < 0.001$; *$P < 0.05$; Kolmogorov-Smirnov test; **a**: $P = 0.02$, sh-control vs sh-Tet1 and $P = 0.01$, sh-control vs sh-Tet2; **b**: $P = 0.01$, EYFP vs Tet1-CD; **c**: $P = 0.00005$, vehicle vs ABT and $P = 0.0005$, vehicle vs CRT; **d**: $P = 0.002$, EYFP vs EYFP + CRT; $P = 0.02$, EYFP vs Tet1-CD; $P = 0.00005$, Tet1-CD vs Tet1-CD + CRT).

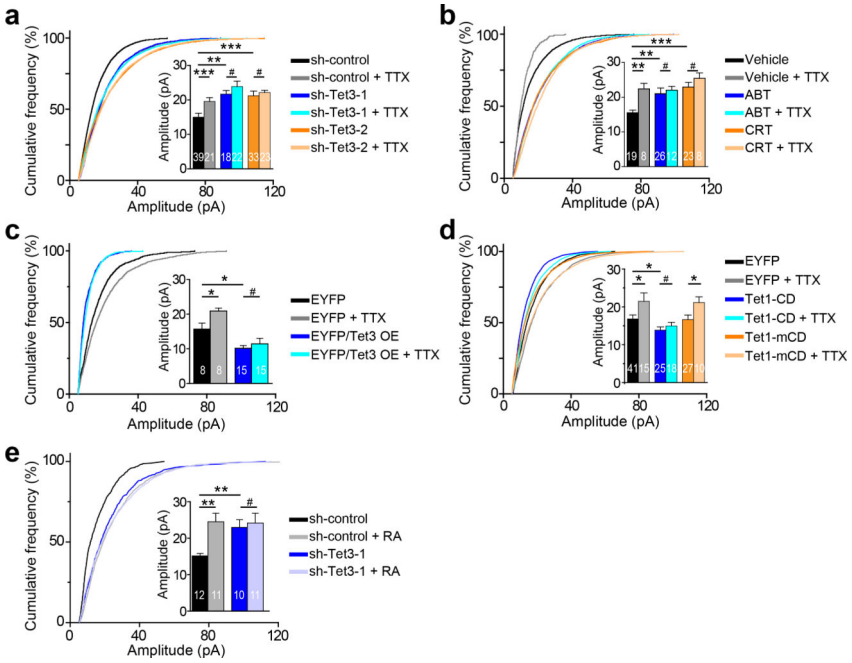

Figure 3.

Tet3 signalling mediates homeostatic synaptic scaling-up of glutamatergic synaptic transmission. (**a-d**) Tet3 signalling mediates TTX-induced synaptic scaling-up. Same as in **Fig. 2**, except that different groups of neurons were treated with TTX (1 μM) for 48 hours before analyses. (**e**) Tet3 KD occludes retinoic acid (RA)-induced synaptic scaling-up. Neurons were infected with AAV to express different shRNAs and were treated with RA (1 μM) for 2 hours before analysis. (***$P < 0.001$; **$P < 0.01$; *$P < 0.05$; $^{\#}P > 0.1$; Kolmogorov-Smirnov test; **a**: $P = 0.0003$, sh-control vs sh-control + TTX; $P = 0.30$, sh-Tet3-1 vs sh-Tet3-1 + TTX; $P = 0.12$, sh-Tet3-2 vs sh-Tet3-2 + TTX; $P = 0.003$, sh-control vs sh-Tet3-1; $P = 0.000009$, sh-control vs sh-Tet3-2; **b**: $P = 0.007$, vehicle vs vehicle + TTX; $P = 0.13$, ABT vs ABT + TTX; $P = 0.26$, CRT vs CRT + TTX; $P = 0.003$, vehicle vs ABT; $P = 0.0005$, vehicle vs CRT; **c:** $P = 0.014$ EYFP vs EYFP + TTX; $P = 0.24$, EYFP/Tet3 OE vs EYFP/Tet3 + TTX; $P = 0.01$ EYFP vs EYFP/Tet3 OE; **d**: P = 0.04, EYFP vs EYFP + TTX; $P = 0.19$, Tet1-CD vs Tet1-CD + TTX; $P = 0.02$, Tet1-mCD vs Tet1-mCD + TTX; $P = 0.01$, EYFP vs TET1-CD; **e**: P= 0.001, sh-control vs sh-control + RA; $P = 0.37$, sh-Tet3-1 vs sh-Tet3-1 + RA; $P = 0.003$, sh-control vs sh-Tet3-1).

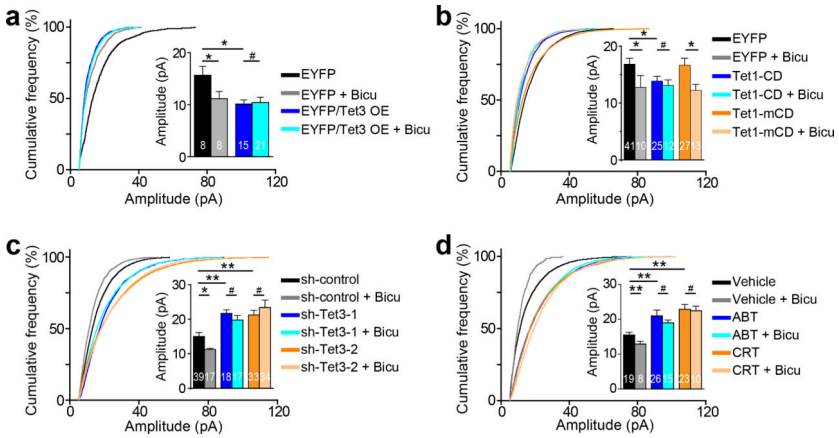

Figure 4.

Tet3 signalling mediates bicuculline-induced homeostatic synaptic scaling-down of glutamatergic synaptic transmission. Same as in **Fig. 3a-d**, except that different groups of neurons were treated with bicuculline (20 μM) for 48 hours before analyses. (***$P < 0.001$; **$P < 0.01$; *$P < 0.05$; $^{\#}P > 0.1$; Kolmogorov-Smirnov test; **a**: $P = 0.03$, EYFP vs EYFP + Bicu; $P = 0.42$, EYFP/Tet3 OE vs EYFP/Tet3 OE + Bicu; $P = 0.01$, EYFP vs EYFP/Tet3 OE; **b**: $P = 0.05$, EYFP vs EYFP + Bicu; $P = 0.28$, Tet1-CD vs Tet1-CD + Bicu; $P = 0.005$, Tet1-mCD vs Tet1-mCD + Bicu; $P = 0.01$, EYFP vs Tet1-CD; **c**: $P = 0.01$, sh-control vs sh-control + Bicu; $P = 0.15$, sh-Tet3-1 vs sh-Tet3-1 + Bicu; P = 0.41, sh-Tet3-2 vs sh-Tet3-2 + Bicu; $P = 0.00001$, sh-control vs sh-Tet3-2; **d**: $P = 0.003$, vehicle vs vehicle + Bicu; $P = 0.13$, ABT vs ABT + Bicu; $P = 0.20$, CRT vs CRT + Bicu; $P = 0.003$, vehicle vs ABT; $P = 0.0005$, vehicle vs CRT).

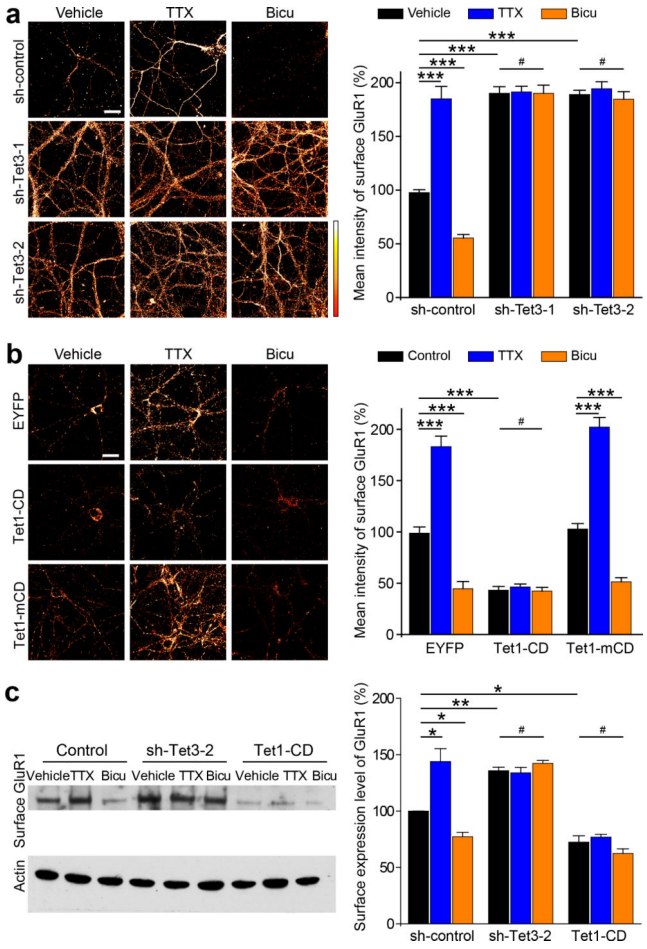

Figure 5.

Tet3 signalling regulates neuronal surface GluR1 levels. (**a**) Tet3 knockdown increases surface GluR1 levels and prevents further changes upon TTX (1 μM) or bicuculline (20 μM) treatment for 48 hours. Shown are sample confocal images of surface GluR1 immunostaining (left, scale bar: 10 μm) and quantification (right). Signal intensity of each condition was normalized to that of neurons expressing sh-control vehicle treatment in parallel cultures. Values represent mean ± s.e.m. (n = 3; **P* < 0.05; #*P* > 0.1; ANOVA). (**b**) Expression of Tet1-CD, but not Tet1-mCD, decreases surface GluR1 levels and prevents further changes upon TTX or bicuculline treatment. Same as in (**a**), except that neurons were infected with AAV to express EYFP, Tet1-CD or Tet1-mCD. (**c**) Western blot analyses of surface GluR1 levels under different conditions. Same as in (**ab**), except that surface biotinylated GluR1 proteins were examined by Western blot and quantified. Full-length blot**s** are presented in Supplementary Figure 11. Values represent mean ± s.e.m. (n = 3; **P* < 0.05; #*P* > 0.1; ANOVA) (**a**: *P* = 0.000001, sh-control vs sh-control + TTX; *P* = 0.000001, sh-control vs sh-control + Bicu; *P* = 0.30, sh-Tet3-1 vs sh-Tet3-1 + TTX; *P* = 0.38, sh-Tet3-1 vs sh-Tet3-1 + Bicu; *P* =0.20 sh-Tet3-2 vs sh-Tet3-2 + TTX; *P* = 0.42, sh-Tet3-2 vs sh-Tet3-2 +Bicu; *P* = NN-A50510B 0.0000001, sh-control vs sh-Tet3-1; *P* = 0.00000001, sh-control vs sh-Tet3-2; **b**: *P* = 0.00000001, EYFP vs EYFP + TTX; *P* = 0.0000001, EYFP vs EYFP + Bicu; *P* = 0.25, Tet1-CD vs Tet1-CD + TTX; *P* = 0.43, Tet1-CD vs Tet1-CD +

Bicu; $P = 0.00000001$, Tet1-mCD vs Tet1-mCD + TTX; $P = 0.00000001$, Tet1-mCD vs Tet1-mCD + Bicu; **c**: $P = 0.03$, sh-control vs sh-control + TTX; $P = 0.01$, sh-control vs sh-control + Bicu; $P = 0.38$, sh-Tet3-2 vs sh-Tet3-2 + TTX; $P = 0.09$, sh-Tet3-2 vs sh-Tet3-2 +Bicu; $P = 0.27$, Tet1-CD vs Tet1-CD + TTX; $P = 0.12$, Tet1-CD vs Tet1-CD + Bicu; $P = 0.004$, sh-control vs sh-Tet3-2; $P = 0.02$, sh-control vs Tet1-CD)

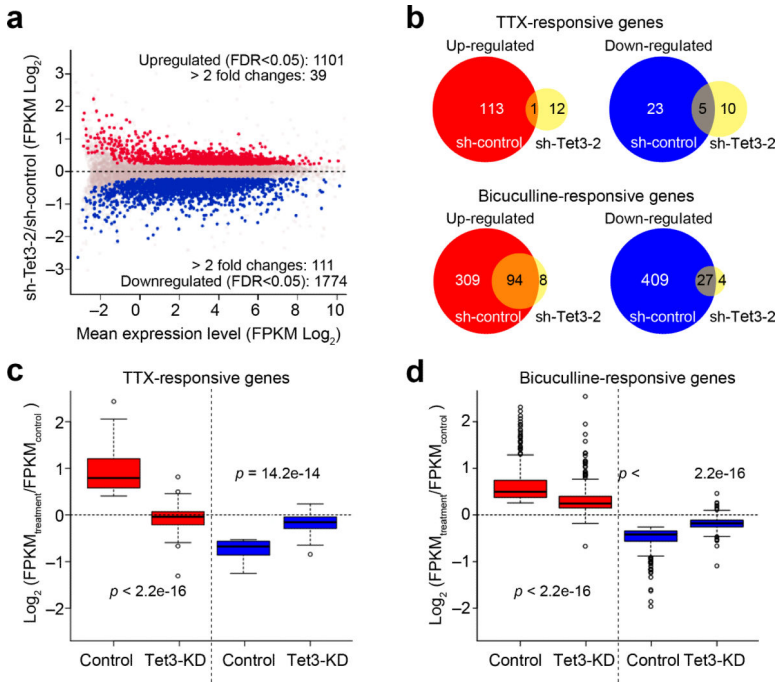

Figure 6.

Tet3 regulates gene expression in neurons in response to global synaptic activity changes. (**a**) Comparison of gene expression in neurons expressing sh-control or sh-Tet3-2 by RNA-seq analyses. Shown is a summary dot plot, with red dots representing up-regulated genes and blue dots representing down-regulated genes (n = 3 samples each; False Discover Rate (FDR) < 0.05). (**b**) Venn diagrams of differentially expressed genes at 4 hours upon TTX (1 μM) or bicuculline (20 μM) treatment in neurons expressing sh-control or sh-Tet3-2 based on RNA-seq analyses (FDR < 0.05). (**c-d**) Box-plot of mean expression levels of up- and down-regulated genes in neurons expressing sh-control in response to TTX (**c**) or bicuculline (**d**) treatment and the expression of the same sets of genes in Tet3-KD neurons under the same condition (Wilcoxon Rank Sum test: **c**: $P = 2.2e^{-16}$, upregulated genes; P = $14.2e^{-14}$ down regulated genes **d**: $P < 2.2e\text{-}^{16}$, both upregulated and down regulated genes.

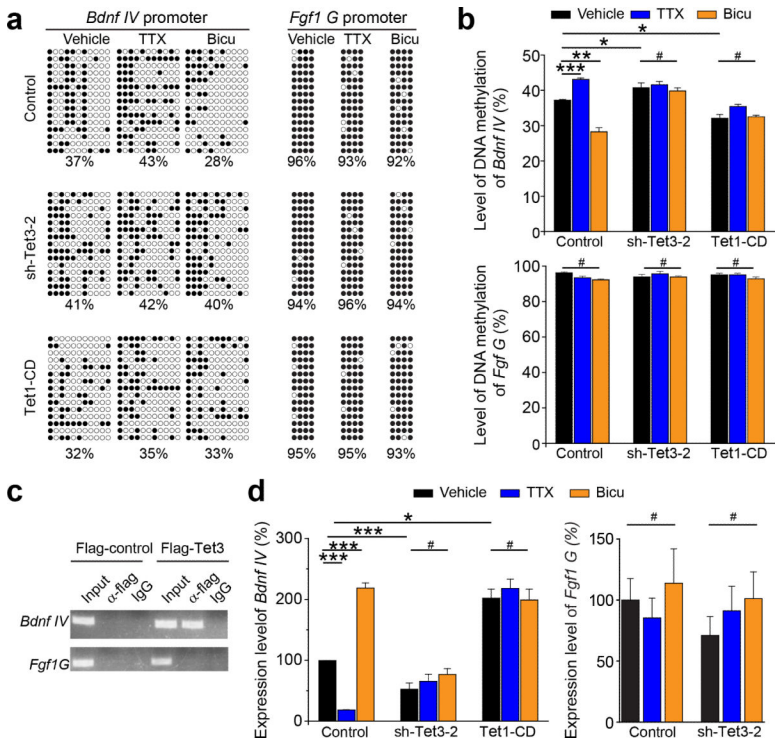

Figure 7.

Essential role of Tet3 in neuronal activity-induced DNA methylation dynamics at the *Bdnf IV* promoter region and gene expression. (**a-b**) Bisulfite sequencing analysis of control, Tet3-KD, or Tet1-CD neurons at 4 hours after treatment of saline, TTX or bicuculline. Sample bisulfite sequencing results at the *Bdnf* promoter IV and *Fgf1G* promoter regions are shown (**a**). Each row represents one allele showing methylation status of individual CpG sites (open circle: unmethylated; closed circle methylated). Mean values of methylate levels of all CpG sites for each region are also shown for each individual culture. A summary of results from multiple cultures is also shown (**b**). A minimum of 15 alleles was examined for DNA methylation for each culture. Values represent mean ± s.e.m. (n = 3-6 cultures; **P* < 0.05; $^{\#}P$ > 0.1; ANOVA; *Bdnf IV*: P = 0.0006, sh-control vs sh-control + TTX; *P* = 0.007, control vs control + Bicu; *P* = 0.10, sh-Tet3-2 vs sh-Tet3-2 + TTX; *P* = 0.32, sh-Tet3-2 vs sh-Tet3-2 + Bicu; *P* = 0.30, Tet1-CD vs Tet1-CD + TTX; *P* = 0.37, Tet1-CD vs Tet1-CD + Bicu; *P* = 0.03, control vs sh-Tet3-2; *P* = 0.02, control vs Tet1-CD). (**c**) ChIP-PCR analyses of Tet3 binding to *Bdnf IV* and *Fgf1G* promoter regions. Flag-tagged Tet3 was expressed in hippocampal neurons for analysis. Full-length blot**s** are presented in Supplementary Figure 11. (**d**) Summary of mRNA expression under different conditions. Values represent mean ± s.e.m. (n = 3 cultures; **P* < 0.05; $^{\#}P$ > 0.1; ANOVA; *Bdnf IV*: *P* = 0.0006, sh-control vs sh-control + TTX; *P* = 0.01, sh-control vs sh-control + Bicu; *P* = 0.16, sh-Tet3-2 vs sh-Tet3-2 + TTX; *P* = 0.07, sh-Tet3-2 vs sh-Tet3-2 +Bicu; *P* = 0.30, Tet1-CD vs Tet1-CD + TTX; *P* = 0.10, Tet1-CD vs Tet1-CD + Bicu; *P* = 0.00004, sh-control vs sh-Tet3-2; *P* = 0.02, sh-control vs Tet1-CD).